

BARITT DIODE VIDEO DETECTORS*

P. J. McCleer and G. I. Haddad
 Electron Physics Laboratory
 Department of Electrical and Computer Engineering
 The University of Michigan
 Ann Arbor, MI 48109

ABSTRACT

The video detection properties of the BARITT diode are described, and experimental and theoretical results for several diode structures are presented. Measured noise equivalent power (NEP) values of less than -99 dBm are reported for a K-band diode in its negative-resistance region. For frequencies beyond those in the negative-resistance region, the detection properties are projected to compare favorably with those of a Schottky-barrier.

Introduction

The nonlinear current-voltage characteristic of the BARITT (barrier injection transit time) diode is proposed as an efficient means for rectification of microwave power. The device differs from the Schottky-barrier diode and the point-contact diode in that it can attain negative resistance from transit-time effects and thus can amplify and detect signals simultaneously. The BARITT diode detector also differs from the negative-resistance tunnel-diode detector as it does not possess the bias instability problems of a dc negative-resistance device, and the BARITT's lack of degenerately doped junctions enable its junction areas to remain tractable even at millimeter wavelengths. This paper presents the initial results of a theoretical and experimental investigation of the BARITT diode video detector.

Theory

The detector model considered in this study is shown in Fig. 1. The impedance transforming-resonating portion of the circuit is shown in a general form, Fig. 1a, and can be characterized by its two-port parameters, in this case its ABCD parameters. At the diode terminals the generator and the resonator-transformer can be replaced by their Thevenin equivalents, Fig. 1b. The BARITT diode series impedance has been divided into three values: a series resistance R_s representing loss in the highly conductive substrate-contact regions of the diode, a forward-biased junction impedance Z_F representing the injecting junction, and a diffusion-drift region impedance Z_B representing the transit-time effects of carrier flow through the reverse-biased junction of the diode. Displacement current capacitive reactances are also included in Z_F and Z_B .

Rectification occurs in the forward-biased junction due to the nonlinear exponential injection process. Rectified current passes through the bias resistor R_o and produces a detectable rectified voltage signal V_R . The rectified current can be computed analytically by expanding the expression for the total particle current through the forward-biased region in a Taylor series about the bias point and extracting the dc component due to the small-signal RF voltage across Z_F . The maximum detected voltage sensitivity γ (V_R at loop resonance normalized to the available power of the generator, with $R_o \gg$ the video resistance of the diode R_V) can then be expressed as

$$\gamma = \frac{4R_g |R_s + R_d|}{|A + CR_g|^2 (R'_g + R_s + R_d)^2} \cdot \frac{|Z_F|^2}{2V_T |R_s + R_d|},$$

where the first term is the efficiency η of the transforming network and the second is the maximum detection sensitivity γ_m of the diode structure itself, independent of any circuit. The diode resistance $R_d = R_F + R_B$ is the real part of $Z_F + Z_B$ at the loop resonance frequency and V_T is the thermal voltage kT/q . At frequencies where R_d becomes negative due to transit-time effects, η can become greater than unity and the diode can effectively amplify and detect simultaneously. Operation in this frequency region is termed "active-mode" detection. Beyond the frequency region of negative resistance the small-signal resistance of the diffusion-drift region R_B remains positive for most devices and falls in magnitude with frequency. The detected voltage responsivity for this "passive mode" can be rewritten as

$$\gamma = \frac{4R_g (R_s + R_d)}{|A + CR_g|^2 (R'_s + R_s + R_d)^2} \cdot \frac{R'_s}{2V_T [\alpha + (f/f_{ce})^2]},$$

where $R'_s = R_s + R_B$, $\alpha = R'_s (1 + R'_s/R_F)/R_F$ and an effective cutoff frequency has been defined $f_{ce} = [2\pi C_F (R_s + R_B)]^{-1}$, where C_F is the depletion layer capacitance of the forward-biased region of the diode. The effective cutoff frequency f_{ce} can be thought of as a figure of merit for the passive-mode BARITT diode detector. Note that f_{ce} is a function of bias and frequency.

Theoretical values for R_d are obtained from an analytical one-dimensional small-signal impedance model that has been developed by the authors for uniformly doped BARITT diode structures. The model is a perturbation on the dc solution for the minority carrier concentration within the base region of the diode. The low-field portion of the drift region is divided into N one-dimensional lumps, each lump having an assumed constant dc minority carrier concentration. Both diffusion and drift current components, based on the difference in concentrations between adjacent lumps and a linear dc electric field variation within each lump, are computed at each lump boundary. The minority carrier concentration within each lump is adjusted until the dc current density across all lump boundaries is equal to a specified value. The ac solution is found in a similar manner, matching boundary conditions at the borders of each lump. The method for obtaining the

* This work was supported by the U. S. Army Research Office under Grant No. DAAG29-76-G-0232.

series impedance of each individual lump is similar to finding the small-signal impedance of the drift region of an IMPATT diode and is fairly standard. As an example of this model, the small-signal resistance for a typical X-band diode (S_i , $p^+ n^+$, base region width = 5 μm , base region doping = $2 \times 10^{15} \text{ cm}^{-3}$) is shown in Fig. 2 as a function of frequency and dc current density.

Experimental and Theoretical Results

Measured maximum detected voltage sensitivities for a $p^+ n^+$ Si diode with a base doping density of $4 \times 10^{15} \text{ cm}^{-3}$, a base width of approximately 3 μm , and a junction area of $2 \times 10^{-5} \text{ cm}^2$ are shown in Fig. 3. The K-band measurements were made with the packaged diode placed in a WR-42 waveguide cavity with a resonant cap structure such that with the addition of an E-H tuner the diode was capable of oscillation at 21 GHz. The Ka-band measurements were made with the same packaged diode placed in a similar WR-28 waveguide cavity with a resonant cap structure such that second-harmonic power could be extracted at 36 GHz. Also shown in Fig. 3 are theoretical sensitivities for the same structure with transformed generator impedance as a parameter. As predicted, the sensitivity within the negative-resistance region could be made arbitrarily high depending upon how close the equivalent generator impedance could be tuned to the total diode negative resistance. Since the resonant cap structure is a fairly high Q as well as a multiply resonant circuit, the E-H tuner was not maximally effective at each frequency in coupling generator power to the diode. To show the relatively narrow-band response of the detector circuit while the diode was in its negative-resistance region, a 100-MHz wide swept measurement was made around a center frequency of 20.5 GHz for a tuning that gave a midband response of $\gamma = 1.8 \times 10^5 \text{ mV/mW}$. As can be seen in Fig. 4 the 3-dB bandwidth was only about 10 MHz. Tuning for less midband gain gave a wider response curve, while tuning for a higher midband gain produced a narrower curve, a typical gain-bandwidth tradeoff. The noise equivalent power (NEP) of the detector was also measured when the signal frequency was in the negative-resistance region of the diode. Similar to the detected voltage sensitivity measurements, seemingly arbitrarily low values of NEP could be measured depending upon one's willingness to accept narrower and narrower frequency response with increasing sensitivity. Typically, stable NEP values of -99 dBm at a video frequency of 1 kHz could be obtained at 20.5 GHz. Still lower values, -109 dBm and below, could be obtained as well but could not be maintained due to bias, tuning, and generator instabilities.

The two experimental points near 35 GHz in Fig. 3 indicate that the BARITT diode can still function as a sensitive detector even at frequencies higher than those within the region of diode negative resistance. This ability is demonstrated in more detail by the results shown in Fig. 5. Here a packaged X-band diode, similar to the one described in Fig. 2, was mounted in the WR-28 waveguide cavity mentioned previously (different resonator cap diameter) and measured as a video detector at 27.4 GHz. The theoretical predictions for γ_m assume

a series resistance of $10^{-5} \Omega\text{-cm}^2$, 10 μm of 0.01 $\Omega\text{-cm}$ substrate (no attempt was made to estimate device-contact resistance). The transforming circuit efficiency was estimated by cavity Q measurements using a shorted diode package to be approximately 40 percent at a diode current of 100 μA .

Theoretical predictions for the millimeter-wave passive-mode detection capabilities for a BARITT diode are given in Fig. 6. Effective cutoff frequencies for a specific structure ($p^+ n^+$, S_i , base region width = 5.0 μm , base region doping = $4.0 \times 10^{15} \text{ cm}^{-3}$, $R_s = 10^{-6} \Omega\text{-cm}^2$) are plotted as functions of signal frequency and diode bias. The transit-time effects on R_B are clearly seen for the higher levels of dc bias. Once the value of R_B falls to a value below that of the fixed series resistance of the substrate contact its effect on f_{ce} is diminished, and the effective cutoff frequency becomes nearly frequency independent. A two-dimensional "honeycomb" version¹ of a BARITT diode passive-mode detector, for devices with emitter diameters comparable to their base region widths, would exhibit even lower $R_s + R_B$ values than those inherent to Fig. 6, due to the current spreading effects of an enlarged collector region. Based on the assumption of a two-dimensional passive-mode detector, effective cutoff frequencies of greater than 10,000 GHz are envisioned for $p^+ n^+$ Si BARITT diodes. Cutoff frequency values in this range would compare to or exceed the highest reported^{2,3} zero-bias cutoff frequencies of GaAs Schottky-barrier devices.

Conclusions

The BARITT diode has been shown both experimentally and theoretically to be an efficient detector of microwave signals. The device negative resistance can be exploited to produce simultaneous amplification and detection resulting in an extremely sensitive though narrow-band detector. Beyond the region of negative resistance the BARITT diode detection sensitivity compares favorably with that of the Schottky-barrier diode. Thus the BARITT structure should be a very useful millimeter wavelength detector.

References

1. Young, D. T. and Irvin, J. C., "Millimeter-Frequency Conversion Using Au-n-Type GaAs Schottky-Barrier Epitaxial Diodes with a Novel Contacting Technique," *Proc. IEEE* (Correspondence), vol. 53, No. 12, pp. 2130-2131, December 1965.
2. McColl, M., Hodges, D. T., and Garber, W. A., "Submillimeter-Wave Detection with Submicron-Size Schottky-Barrier Diodes," *IEEE Trans. on Microwave Theory and Techniques*, vol. MTT-25, No. 6, pp. 463-467, June 1977.
3. Schneider, M. V. and Carlson, E. R., "Notch-Front Diodes for Millimeter-Wave Integrated Circuits," *Electronics Letters*, vol. 13, No. 24, pp. 745-747, November 24, 1977.

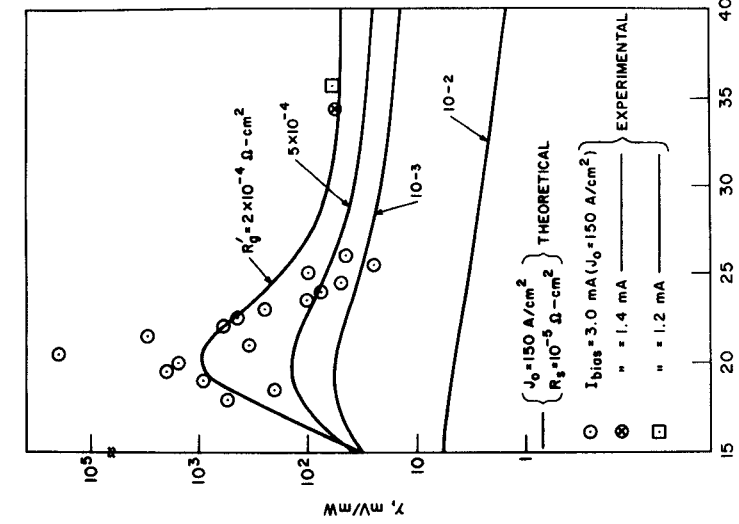


FIG. 1(a)

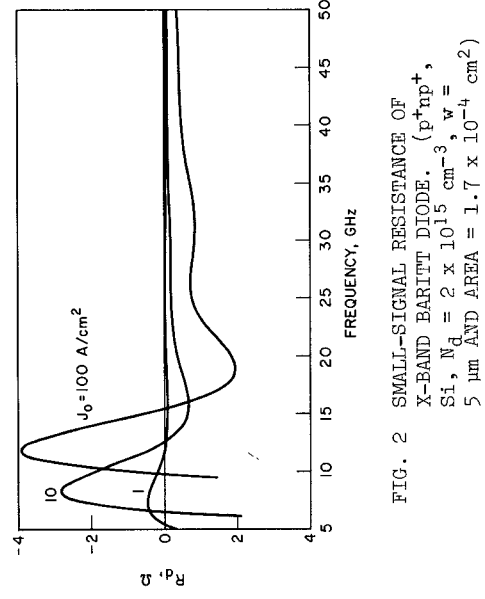


FIG. 2 SMALL-SIGNAL RESISTANCE OF X-BAND BARITT DIODE. (p^+np^+ , Si, $N_d = 2 \times 10^{15} \text{ cm}^{-3}$, $W = 5 \mu\text{m}$ AND AREA = $1.7 \times 10^{-4} \text{ cm}^2$)

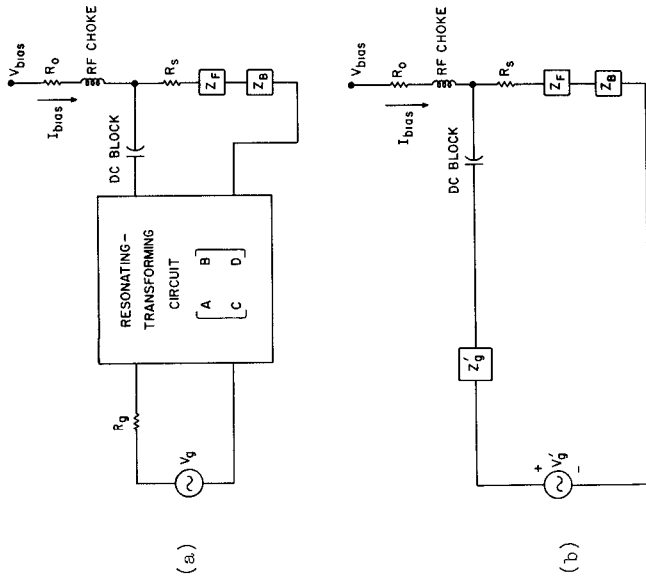


FIG. 1 BARITT DIODE DETECTOR CIRCUITS. (a) DETECTOR CIRCUIT AND (b) THEVENIN EQUIVALENT CIRCUIT. $V_g^* = V_g / (A + CR_g)$ AND $Z_g^* = (B + DR_g) / (A + CR_g)$

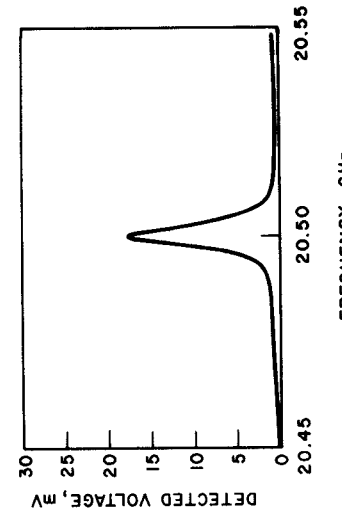


FIG. 4 SWEPT FREQUENCY DETECTOR RESPONSE IN NEGATIVE-RESISTANCE FREQUENCY REGION.

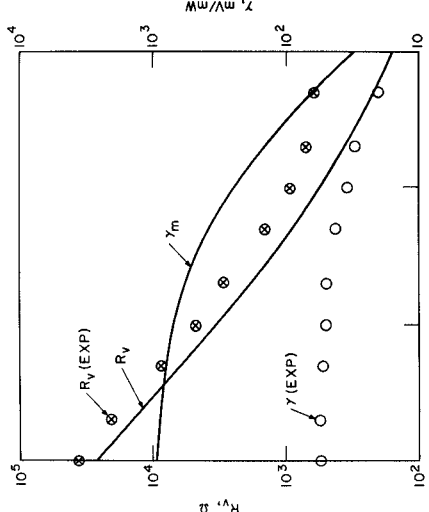


FIG. 5 THEORETICAL AND EXPERIMENTAL RESULTS FOR VIDEO DETECTION AT 27.44 GHz WITH X-BAND DIODE.

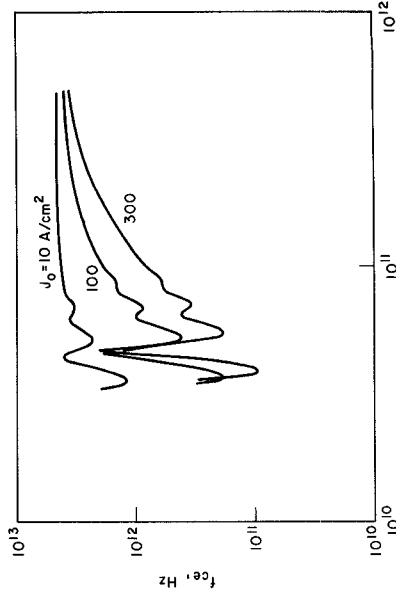


FIG. 3 EXPERIMENTAL AND THEORETICAL DETECTED VOLTAGE SENSITIVITY FOR A K-BAND BARITT DIODE.



FIG. 6 EFFECTIVE CUTOFF FREQUENCIES AS A FUNCTION OF BIAS FOR A p^+np^+ Si BARITT DEVICE.